




Biofilm thickness restraint carriers enhance free nitrous acid inhibition for partial nitrification

Alexander Schopf ^a, Magnus Christensson ^b, Maria Piculell^b, Xin Tian^a and Robert Delatolla ^{a,*}

^a Department of Civil Engineering, University of Ottawa, Ottawa, Canada

^b Veolia Water Technologies, AnoxKaldnes, Sweden

*Corresponding author. E-mail: robert.delatolla@uottawa.ca

 AS, 0000-0002-8441-5371; MC, 0000-0001-5973-8315

ABSTRACT

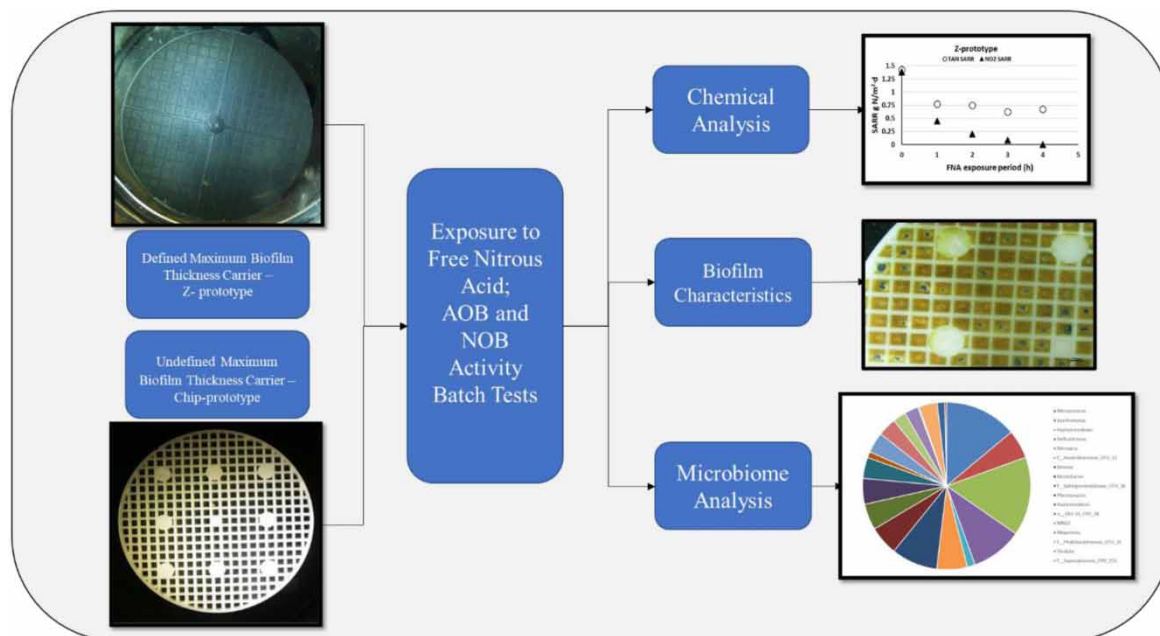
Ammonia is a deleterious pollutant present in municipal wastewater that can be hazardous if released into the environment. There is a need for the development of novel processes to advance ammonium removal technologies. Partial nitrification (PN) and anaerobic ammonia oxidation (anammox) are modern treatment processes that can be combined to provide energy-efficient ammonia removal; however, these processes have been shown to be challenging to implement as a two-stage system. New methods to achieve steady PN need to be discovered. Free nitrous acid (FNA) exposure has been explored as a possible strategy for achieving PN; however, exposure time to FNA and FNA dosage is dependent on the treatment system. For biofilm technologies, such as the moving bed biofilm reactor and biofilm characteristics, including biofilm thickness, can cause inconsistent results. Therefore, this study compares defined maximal biofilm thickness with undefined biofilm thickness and their capacity to achieve PN using FNA. This study found that a defined maximal biofilm thickness designed carrier maintained a thin biofilm capable of achieving PN after FNA exposure while the undefined biofilm thickness designed carrier was not suitable for stable PN.

Key words: biofilm thickness, defined biofilm thickness, free nitrous acid, MBBR, partial nitrification

HIGHLIGHTS

- There is a need for new and robust strategies to achieve stable partial nitrification using attached-growth technologies.
- Thin biofilm has shown potential for enhanced free nitrous acid (FNA) inhibition of nitrite-oxidizing bacteria (NOB) activity.
- Maximal biofilm thickness and undefined thickness carriers studied for FNA inhibition.
- Maximal biofilm thickness carriers show NOB inhibition at 3 h of FNA exposure.
- Undefined thickness carriers are not capable of achieving NOB inhibition with FNA exposure.

GRAPHICAL ABSTRACT



INTRODUCTION

Nitrogen, specifically in the form of ammonium and ammonia, which is collectively referred to as total ammonia nitrogen (TAN), can be harmful to the natural environment including bodies of water such as rivers, lakes, and oceans. A primary source of TAN discharge to receiving waters is the effluent from municipal wastewater resource recovery facilities (WRRF). To avoid discharging nitrogen into the environment, raw wastewater undergoes various treatment processes. The conventional TAN treatment consists of the nitrification process followed by the denitrification process. Nitrification is the autotrophic, aerobic oxidation of TAN to nitrite and nitrate, while denitrification is the heterotrophic, anoxic reduction of nitrate to nitrogen gas by organic carbon. Nitrification and denitrification lack synergy as the nitrification process can be inhibited by organic carbon, while the subsequent denitrification process requires an organic carbon source. The addition of external organic carbon sources to achieve the commonly installed post-anoxic denitrification results in additional costs.

Nitrification is a two-step process consisting of nitrification, the oxidation of TAN to nitrite by ammonia-oxidizing bacteria (AOB), and is conventionally the rate limiting step (Lotfi *et al.* 2019); and nitratation, the oxidation of nitrite to nitrate by nitrite-oxidizing bacteria (NOB). Modern nitrogen removal is the combination of partial nitrification (PN) and anaerobic ammonia oxidation (anammox) and has been demonstrated to have the capacity to adequately treat nitrogen in both side-stream and mainstream wastewater treatment. PN is the oxidation of a portion of TAN to nitrite while maintaining as little nitrate production as possible as a pretreatment for anammox, whereas the anammox process is the anoxic oxidation of TAN by nitrite (Strous *et al.* 1998). The combined PN and anammox (PN/A) processes requires 60% less oxygen, requires no additional carbon source, and produces 90% less biomass than conventional nitrification and denitrification and therefore have significant economic benefits (Mulder 2003; Van Loosdrecht & Salem 2006; Siegrist *et al.* 2008). PN/A can be performed in a single reactor system or in a multiple reactor system. Single reactor systems, such as the DEMON (Shalini & Joseph 2012), CANON (Wang *et al.* 2013), and ANITA™ Mox systems (Christensson *et al.* 2013), operate at low dissolved oxygen (DO) concentrations as anammox bacteria are inhibited by DO (above 0.5 mg O₂/L). At low DO concentrations, the anammox bacteria are capable of outcompeting the NOB for nitrite (Strous *et al.* 1998; Third *et al.* 2005). At TAN concentrations typical to mainstream and sidestream wastewater treatment, nitritation is oxygen rate-limited (Rusten *et al.* 2006); therefore, operating at low DO concentrations required for anammox treatment results in low PN rates, and so, combined PN/A systems require larger operating volumes to compensate for the lower rates of PN.

Multi-reactor systems that split the PN and anammox processes into different reactors can be optimized for each of the distinct processes, resulting in higher nitrification and anammox rates. However, there have been difficulties shown in the suppression of NOB activity, which resulted in the development of various control strategies to suppress NOB activity. NOB activity control strategies that have been implemented to achieve NOB suppression in PN reactors include operating with DO restriction, alkalinity restriction, sequencing batch operations, chemostat operations (no solids retention), and NOB inhibition through free ammonia (FA) and free nitrous acid (FNA) (Hellings *et al.* 1998; Fux *et al.* 2004; Lackner *et al.* 2014; Dosta *et al.* 2015; Gilbert *et al.* 2015; Piculell *et al.* 2016a, 2016b; Duan *et al.* 2019).

FA and FNA have been shown to be inhibitory to both AOB and NOB, and NOB have demonstrated greater sensitivity to FA and FNA than AOB (Anthonisen *et al.* 1976). Exposure to FA and FNA to achieve PN has been accomplished through elevated TAN and nitrite concentrations from sidestream centrate that typically have elevated TAN and nitrite concentrations compared to mainstream municipal wastewaters (Lackner *et al.* 2014). The TAN and nitrite concentrations present in typical municipal wastewaters are insufficient at typical municipal temperatures and pH values to inhibit NOB. Periodic exposure of the bacteria in the mainstream system to sidestream wastewater has been investigated as a strategy to inhibit NOB, through exposure to elevated FA and FNA concentrations, by either periodically changing the feed or transporting the biomass to a point of contact with sidestream wastewater (Lemaire *et al.* 2014; Wang *et al.* 2014; Piculell *et al.* 2016b).

Planktonic and sessile technologies have both been shown to be able to achieve PN; however, sessile technologies have various advantages over planktonic technologies such as lower sludge production, longer solids retention, and a smaller land footprint. The moving bed biofilm reactor (MBBR) is a sessile technology that consists of a tank that is filled with carriers with attached biofilm and the carriers moving through the bulk liquid. High-density polyethylene carriers have been used as carriers in MBBR systems and many carrier geometries have been developed to optimize aspects such as size, loading rate, surface area, and potential biofilm thickness. Carriers designed to control biofilm thickness have been used to compare a thin biofilm to a thicker biofilm, and the thin biofilm has been shown to enhance the inhibition of NOB activity using periodic exposure to high strength wastewater compared to a thicker biofilm (Piculell *et al.* 2016b). This work studies the potential for the use of carriers with defined maximal biofilm thickness to be used for improved PN performance. A current gap of knowledge exists with respect to the direct comparison of defined maximal biofilm thickness designed carriers to undefined biofilm thickness designed carriers, based on carrier geometry, for the purpose of NOB population growth or activity inhibition and enhanced PN.

In this study, the AnoxK™ Z-style carrier (z-prototype) and the AnoxK™ M-style prototype carrier (chip-prototype) are used to compare a carrier designed to define a maximal biofilm thickness (z-prototype) and a carrier that was not designed to define a biofilm thickness (chip-prototype) for PN. This study aims to compare defined and undefined maximal biofilm thickness for achieving PN using intermittent exposure to FNA to inhibit NOB activity or population growth. This study also aims to determine the effect of the length of FNA exposure on nitrification and nitrification inhibition with both defined and undefined maximal biofilm thickness. The biofilm characteristics and microbiome are analyzed to compare the z-prototype and the chip-prototype.

METHODS AND MATERIALS

Carrier geometry

To quantify the effects of maximum defined biofilm thickness compared to undefined maximum biofilm thickness on FNA inhibition to achieve PN, two carrier types were used: the z-prototype and the chip-prototype. The z-prototype carriers and the chip-prototype carriers are not commercially available at the time of writing. The z-prototype (Supplementary Fig. S1) is a thin, flat, solid disk with a diameter of 31 mm, small, 50 μm high walls hatched on each side and a specific surface area of 1200 $\text{m}^2/10^6$ carriers. The 50 μm walls protect the biofilm that is within the small cells; however, the biofilm that grows outside of the walls is eroded and detached, thus maintaining a thin biofilm with a maximum defined biofilm thickness of 50 μm . The chip-prototype (Supplementary Fig. S2) is a thin disk with a diameter of 31 mm that has many carrier pores, and a specific surface area of the chip-prototype is 1100 $\text{m}^2/10^6$ carriers. The biofilm grows within the carrier pores; however, the biofilm growth is unrestricted within the carrier-pore and, while the carrier is designed to maintain the biofilm thickness within a certain range, the carrier does not maintain a consistent thickness; therefore, the maximum biofilm thickness is undefined. As the z-prototype was designed to maintain an exceptionally thin biofilm, it will be referred to as the thin biofilm carrier, and while the chip-prototype does not necessarily have a thick biofilm, the undefined biofilm thickness design of the

carrier allows a thicker biofilm than that on the z-prototype to develop; thus, the chip-prototype will be referred to as the thick biofilm carrier.

Batch test protocol and set-up

To quantify the impact of FNA exposure contact time and carrier design choices, a series of batch tests were performed. The impact of each test condition was quantified through two batch tests: a nitrification batch test to determine NOB activity, followed by a denitrification batch test to determine AOB activity. The order of batch tests is to individually quantify the effects of exposure time on NOB and AOB separately. Denitrification produces nitrite which would provide substrate to the NOB and potentially allow the NOB to be active prior to the nitrification batch test; thus, the denitrification batch test would need to be performed prior to the nitrification batch test. Singleton reaction rate tests were performed.

To perform the batch tests, 20 carriers of the same design (either thin or thick biofilm carrier) were extracted from the maintenance reactor and lightly rinsed with distilled water. The carriers were then placed into the FNA reactor for 0, 1, 2, 3, or 4 h. The 0-hour exposure was used to quantify the uninhibited AOB and NOB activities and establish baseline values to compare to the inhibition batch trial data. After the target exposure time, the carriers were removed from the FNA exposure solution and gently rinsed with distilled water to remove any excess exposure solution.

The batch reactor was filled with 500 mL ($h = 15$ cm) of the nitrification test solution, and the carriers were added. A 1.5 mL sample was taken simultaneously to the addition of the carriers at $t = 0$ min. The batch test took place over a 2-h period with the extraction of 1.5 mL samples occurring every 20 min. After the last sample was taken, the carriers were removed and rinsed gently in distilled water, and the reactor was emptied and rinsed. The reactor was then filled with 500 mL of denitrification solution and the carriers were re-added. A 1.5 mL sample was taken as the carriers were added as $t = 0$ min. Samples with a volume of 1.5 mL were taken every 20 min over a 2-h period. The carriers were disposed of after batch testing. The TAN and $\text{NO}_2\text{-N}$ concentrations and associated nitrogen balances from the batch tests for the thin and thick biofilm carriers are presented in Supplementary Tables S.1–S.8, respectively.

The batch reactor (Supplementary Fig. S3) was a single 2 L glass reactor with a temperature-controlled water jacket. The batch reactor was operated at a constant temperature of 20 °C using the temperature control water jacket. DO was maintained at constant 4 mg/L through oxygen and nitrogen bubbled in from the bottom of the reactor at a combined flow rate of 1 L/min to provide consistent mixing. The pH was maintained at 7.5 through consistent monitoring and adjustment using 0.05 M H_2SO_4 or 0.05 M NaOH.

The FNA reactor was a single 8 L metal reactor with a temperature-controlled water jacket. The reactor was filled with 5 L of FNA exposure solution and operated at a temperature of 30 °C and a pH of 6. The pH was controlled using a buffer solution and titrated using 1 M H_2SO_4 and 1 M NaOH. Aeration was provided at a rate of 0.5 L/min to promote movement within the reactor. The reactor operated with a TAN concentration of 400 mg TAN/L and a nitrite concentration of 500 mg $\text{NO}_2\text{-N/L}$, providing an FNA concentration of 0.88 mg N/L.

Carrier preparation and maintenance

The thin and thick biofilm carriers were prepared and maintained in an 8 L metal reactor. The temperature was maintained using a temperature-controlled jacket attached to a hot water bath. Large bubble aeration was provided through the bottom of the reactor to provide oxygen and mixing. The aeration was hydrated by bubbling the air through water to prevent water vaporization within the reactor. The reactor was fed at a rate of 81.6 L/d with a solution that was made from diluted high strength waste water, providing an influent TAN concentration of 43.7 ± 1.1 mg/L and an average surface area loading rate (SALR) of 2.83 ± 0.05 g TAN/m²·d. The maintenance reactor operated at a DO of 6 mg/L and a pH of 7.8 ± 0.2 mg/L.

The maintenance reactor was initially filled with unseeded thin and thick biofilm carriers and seeded using the effluent from a nitrifying MBBR system and sludge from a nitrifying activated sludge system. The maintenance reactor was initially operated at an SALR of 0.9 g TAN/m²·d and a temperature of 25 °C to facilitate biofilm growth. The SALR was increased to 2.5 ± 0.03 g TAN/m²·d over the course of 2 weeks. After a further 2 weeks of operation, the temperature was reduced to 20 °C to simulate municipal treatment and the SALR was further increased to 2.83 ± 0.05 g TAN/m²·d as carriers were removed for a separate study.

Feed solution

The wastewater feed solution for the system consisted of centrate from the Sjölanda wastewater treatment plant, containing approximately 1030 mg TAN/L and 1170 mg $\text{CaCO}_3\text{/L}$, that was diluted to an average of 43.7 ± 1.1 mg TAN/L using tap

water. The average influent nitrite concentration was 1.34 ± 0.59 mg NO_2^- -N/L. To ensure that there was sufficient alkalinity, 300 mg CaCO_3 /L as NaHCO_3 was added for a total of approximately 350 mg CaCO_3 /L. Due to the use of centrate as the basis for the feed, additional nutrients and carbon were not added. Centrate contained 257 mg sCOD/L, 147 mg BOD_7 /L, and 330 mg TSS/L (Christensson *et al.* 2013). As centrate contains organic matter and bacteria, any chemical parameters in the tap water used for dilution would be negligible, and any residual chlorine is assumed to have been consumed.

The FNA exposure solution consisted of 7.642 g NH_4Cl (1.5284 g/L), 12.321 g NaNO_2 (2.4642 g/L) as substrates, and 68 g KH_2PO_4 (13.6 g/L) as a buffer dissolved in 5 L of distilled water resulting in concentrations of 400 mg NH_4^+ -N/L and 500 mg NO_2^- -N/L, with KH_2PO_4 acting as a buffer to keep the pH stable.

The nitrification kinetic test solution for the baseline and the inhibition tests consisted of 1.125 g of NaHCO_3 , 0.2218 g of NaNO_2 , and 0.4 mL of PO_4 solution (12.75 g P/L) dissolved in 1.5 L of distilled water. The nitrification kinetic test solution had a substrate concentration of 30 mg NO_2^- -N/L.

The nitrification kinetic solution for the baseline and the inhibition tests consisted of 1.125 g of NaHCO_3 , 0.257 g of NH_4Cl , and 0.4 mL of PO_4 solution (12.75 g P/L) dissolved in 1.5 L of distilled water. The nitrification kinetic test solution had a substrate concentration of 45 mg NH_4^+ -N/L. The solutions were titrated to a pH of 7.5 using 0.5 M H_2SO_4 .

Chemical analysis methods

Chemical analyses for batch test TAN, nitrite, and nitrate concentrations were performed using HACH vial test kits: Ammonia LCK 303, Nitrite LCK 342, and Nitrate LCK 339, respectively (HACH, CO, USA). To compensate for the interference of nitrite on the Nitrate LCK 339 HACH test, a standard curve was developed and a correction factor of $0.31 \times [\text{mg NO}_2^-/\text{N/L}]$ was subtracted from the corresponding nitrate value.

Biofilm mass acquisition and analysis

Biofilm mass was quantified using a modified version of the method used in Piculell *et al.* (2016a) and Young *et al.* (2017). Twenty carriers were extracted from the continuous reactor, placed in an aluminum weighing dish, and dried at 105 °C for a minimum of 8 h. After this period, the carriers were cooled in a desiccator for a minimum of 1 h. Once the carriers were cooled to room temperature, the carriers and the weighing boat were weighed. The carriers were removed from the weighing boat and placed in 500 mL of 1 M NaOH for a minimum of 8 h. The carriers were rinsed with distilled water and gently scrubbed with a soft bristle brush to ensure all of the biofilm was removed. The rinsed carriers were returned to the same aluminum weighing boat as before and dried in an oven at 105 °C for a minimum of 8 h. After this period, the carriers and weighing boat were placed in the desiccator for a minimum of 1 h and weighed. The difference in weight was the weight of the biofilm removed. The weight of the biofilm removed was divided by 20 to obtain the average biofilm mass of the carrier.

Biofilm thickness image acquisition and analysis

To quantify the thickness of the biofilm and analyze the biofilm morphology, images were taken using the OLYMPUS SZ-ET (Olympus Corporation, Japan) and analyzed using the ImageJ program (LOCI University of Wisconsin, USA). To quantify the thickness of the chip-style carriers, eight top-down images at $2\times$ magnification were acquired. The length of one side of the carrier pores was used to set the scale for the ImageJ program and over 200 biofilm measurements were taken. The results were exported into Microsoft Excel where the results were analyzed. To quantify the biofilm thickness of the z-style carriers, the carriers were cut in half and oriented such that the inside of the carrier was directed toward the camera. Ten images were acquired at $8\times$ magnification with added scale bars. The ImageJ program was used to quantify biofilm thickness using a minimum of 150 individual measurements.

Microbiome acquisition and analysis

To quantify the microbiome, two 1.5 mL Eppendorf tubes per carrier per condition were filled with fresh biofilm extracted from carriers obtained from the continuous flow reactor. The samples were labeled and stored in a -30 °C freezer until further analysis.

The samples were analyzed by DNASense (Aalborg, Denmark) with the 16S rRNA gene amplicon sequencing targeting the V1–3 bacterial variable region. The raw sequencing data were processed at DNASense using the UPARSE workflow (Edgar 2013). Data were analyzed through Rstudio using the ampvis2 package (Aalborg University, Denmark) and the MiDAS database. The subsequent sections describe the protocol used by DNASense (Denmark).

DNA extraction

The standard protocol for the FastDNA Spin kit for Soil (MP Biomedicals, USA) was used for DNA extraction. The following exceptions to the standard protocol were applied: 120 μL of MT buffer, 500 μL of the sample, and 480 μL of sodium phosphate buffer were added to the Lysing Matrix E tube; DNA concentration was quantified using the Qubit dsDNA HS/BR Assay kit (Thermo Fisher Scientific, USA); bead beating was performed at 6 m/s for four sets of 40 s (Albertsen *et al.* 2015); and to validate the purity of a subset of DNA extracts and the product size, gel electrophoresis was used using TapeStation 2200 and Genomic DNA screentapes (Agilent, USA).

Library preparation

A custom protocol based on Caporaso *et al.* (2012) was used to prepare the bacteria 16S V1–3 rRNA gene sequencing libraries. To make a template for the PCR amplification of the bacteria 16S V1–3 rRNA gene amplicon, up to 10 ng of extracted DNA was used. Each 25 μL PCR contained 1.5 mM of MgSO_4 , 100 μM of each dNTP, Platinum High Fidelity buffer (1 \times) (Thermo Fisher Scientific, USA), 400 nM of each forward and reverse barcoded library adaptors, and 0.5 U of Platinum Taq DNA polymerase HF. The PCR was conducted with the following program: initial denaturation at 95 $^\circ\text{C}$ for 2 min, 30 cycles of amplification (95 $^\circ\text{C}$ for 20 s, 56 $^\circ\text{C}$ for 30 s, 72 $^\circ\text{C}$ for 60 s), and a final elongation at 72 $^\circ\text{C}$ for 5 min. For each sample, duplicate PCRs were performed and after the PCR the duplicates were pooled. The adaptors contain 16S V1–3 specific primers: [27F] AGAGTTTGTATCCTGGCTCAG and [534R] ATTACCGCGGCTGCTGG (Jumpstart Consortium. 2012). The standard protocol for Agencourt Ampure XP Beads (Beckman Coulter, USA) was used to purify the resulting amplicon libraries with a sample to bead ration of 5:4. The DNA was eluted to 25 μL of nuclease-free water (Qiagen, Germany). A Qubit dsDNA HS Assay kit (Thermo Fisher Scientific, USA) was used to measure the DNA concentration and gel electrophoresis was used to validate the product size and purity of a subset of the sequencing library. Gel electrophoresis was performed using TapeStation 2200 and D1000/High sensitivity D1000 screentapes (Agilent, USA).

DNA sequencing

The purified sequencing libraries were diluted to 6 nM after being pooled in equimolar concentrations. A Miseq (Illumina, USA) was used to pair-end sequence the samples (2 \times 300 bp) using a MiSeq Reagen kit v3 (Illumina, USA) following the standard guidelines for preparing and loading samples on the MiSeq. To overcome low complexity issues with amplicon samples, a >10% PhiX control library was spiked in.

Bioinformatic processing

The Trimmomatic v.0.32 (Bolger *et al.* 2014), using settings of MINLEN:275 and SLIDINGWINDOW:5:3, was used to trim the forward and reverse reads. The trimmed forward and reverse reads were merged using FLASH v.1.2.7 (Magoč & Salzberg 2011) with the settings – m 10 – M 200. The UPARSE workflow (Edgar 2013) was used to dereplicate and format the trimmed reads. The dereplicated reads were clustered using the usearch v.7.0.1090 –cluster_otus command with default settings. OUT abundances were estimated using the usearch v.7.0.1090 –usearch_global command with –id 0.97 –maxaccepts 0 –maxrejects 0. The RDP classifier (Wang *et al.* 2007) was implemented in the parallel_assign_taxonomy_rdp.py script in QIIME (Caporaso *et al.* 2010) and was used to assign the taxonomy, using –confidence 0.8 and the MiDAS database v.123 (McIlroy *et al.* 2017), which is a curated database based on the SILVA database, release 123 (Quast *et al.* 2013). The results were analyzed using the ampvi package v.2.4.10 (Albertsen *et al.* 2015) in R v.3.5.1 (R Core Team 2017) using the Rstudio IDE.

Batch test surface area removal rate

The surface area removal rate (SARR) for the baseline and inhibited batch tests was calculated using the following equation:

$$SARR_{batch\ test} = \frac{V \times (C_0 - C_t)}{SA_{carrier} \times t} \quad (1)$$

where V is the volume of solution, C_0 is the concentration of substrate at $t = 0$, C_t is the concentration of substrate at $t = t$, $SA_{carrier}$ is the combined surface area of all of the carriers in the vessel, and t is the time that has passed during the batch test.

For the batch tests: $V = 0.5\ \text{L}$; $C_0 = 45\ \text{mg TAN/L}$ or $30\ \text{mg NO}_2\text{-N/L}$; C_t is the concentration at time t ; $SA_{carrier} = 0.024\ \text{m}^2$ for the thin biofilm carrier or $0.022\ \text{m}^2$ for the thick biofilm carrier; and $t =$ time at which the sample was taken (0–0.0833 d).

Percent inhibition

Percent inhibition is defined by the fraction of baseline activity that is demonstrated after exposure to the synthetic exposure solution:

$$\text{Percent Inhibition} = \frac{SARR_{\text{Baseline}} - SARR_{\text{Inhibited}}}{SARR_{\text{Baseline}}} \times 100\% \quad (2)$$

where $SARR_{\text{Baseline}}$ is the TAN or NO_2^- -N SARR quantified from the kinetic batch tests using carriers that were not exposed to the synthetic exposure solution, and $SARR_{\text{Inhibited}}$ is the TAN or NO_2^- -N SARR quantified from the kinetic batch tests using carriers that were exposed to the synthetic exposure solution for a set period of time.

RESULTS AND DISCUSSION

Batch test kinetics

Batch kinetic testing was used to quantify the effects of FNA exposure time on nitrifying biofilms at 20 °C for the thin biofilm carriers and the thick biofilm carriers. This is to quantify the effects of biofilm thickness control strategies on AOB and NOB inhibition due to FNA. The SARR of the thin and thick biofilm carriers for both nitrification and nitratation are shown in Figure 1 and Table 1. The baseline AOB nitrification kinetic rates (TAN SARR) were 1.43 ± 0.05 and 2.56 ± 0.09 g TAN/m²·d for the thin and thick biofilm carriers, respectively, and the baseline NOB nitratation kinetic rates (NO_2^- -N SARR) were 1.39 ± 0.06 and 6.05 ± 0.28 g NO_2^- -N/m²·d for the thin and thick biofilm carriers, respectively. Note that as the nitrification and nitratation kinetics were determined separately, using solutions that contain either ammonia or nitrite, the nitratation rates were not limited by the nitrification rates as would normally be seen in conventional nitrification. The thick biofilm carrier had higher baseline TAN and NO_2^- -N SARR kinetic rates than the thin biofilm carrier, similar to what was seen when comparing carriers of different thicknesses (Suarez *et al.* 2019). The thick biofilm carrier also displayed greater overall resilience to FNA exposure than the thin biofilm carrier. Although the thin and thick biofilm carriers experienced similar NO_2^- -N SARR percent inhibition, the higher baseline NO_2^- -N SARR of the thick biofilm carrier meant that significant nitratation (1.68 ± 0.08 g NO_2^- -N /m²·d) was

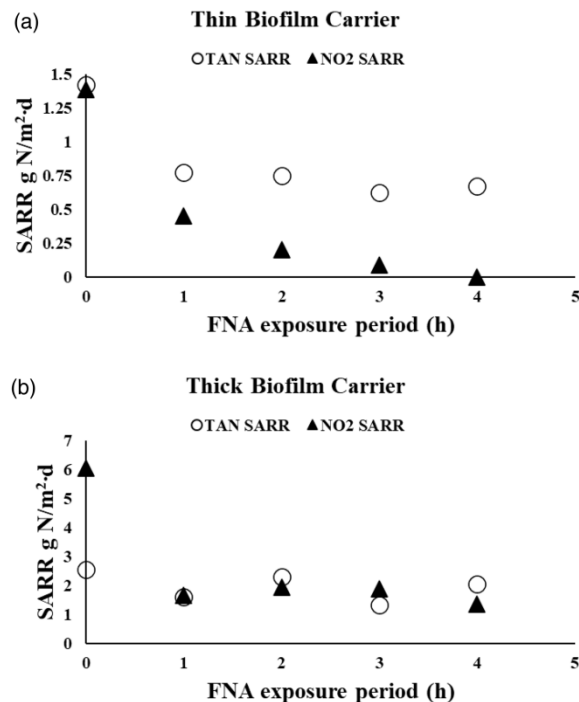


Figure 1 | Nitritation (AOB) removal rates (○) and nitratation (NOB) removal rates (▲) for thin biofilm carrier (a) and thick biofilm carrier (b).

Table 1 | Nitritation (AOB) removal rates and inhibition percentage, and nitratation (NOB) removal rates and inhibition percentage for the thin biofilm carrier and the thick biofilm carrier

	TAN SARR (g TAN-N/m ² -d)	TAN SARR inhibition (%)	NO ₂ ⁻ -N SARR (g NO ₂ ⁻ -N/m ² -d)	NO ₂ ⁻ -N SARR inhibition (%)
<i>Thin biofilm carrier</i>				
Baseline	1.43 ± 0.05	–	1.39 ± 0.06	–
1 h	0.78 ± 0.03	45.61 ± 1.7	0.45 ± 0.02	67.57 ± 3.1
2 h	0.75 ± 0.03	47.47 ± 1.7	0.20 ± 0.01	85.59 ± 3.9
3 h	0.625 ± 0.02	56.14 ± 2.1	0.09 ± 0.004	93.69 ± 4.3
4 h	0.675 ± 0.24	52.63 ± 1.9	0.0 ± 0	100.0 ± 0
<i>Thick biofilm carrier</i>				
Baseline	2.56 ± 0.09	–	6.05 ± 0.28	–
1 h	1.61 ± 0.06	37.23 ± 1.4	1.68 ± 0.08	72.3 ± 3.3
2 h	2.32 ± 0.08	9.57 ± 0.4	1.94 ± 0.09	68.02 ± 3.1
3 h	1.32 ± 0.05	26.6 ± 1.0	1.88 ± 0.09	68.15 ± 3.1
4 h	2.04 ± 0.07	20.21 ± 0.7	1.36 ± 0.06	77.48 ± 3.6

still occurring. Furthermore, beyond the NO₂⁻-N SARR inhibition experienced at 1 h of exposure, the thick biofilm carrier NO₂⁻-N SARR was not correlated with exposure time, and even after 4 h of exposure, the NO₂⁻-N SARR inhibition was 77.5% with an NO₂⁻ SARR of 1.36 ± 0.06 g NO₂⁻-N /m²-d, which is still a significant NO₂⁻-N SARR. Both the thin and thick biofilm carriers experienced TAN SARR inhibition after 1 h of exposure, and while the thin biofilm carrier had a moderate trend of increased TAN SARR inhibition with exposure time, there was no correlation between TAN SARR inhibition and exposure time for the thick biofilm carrier. The optimal exposure time for the z-prototype was 3 h as the NO₂⁻-N SARR was 0.09 ± 0.004 g NO₂⁻-N/m²-d, with an NO₂⁻-N SARR inhibition of 94% which is sufficient for PN; however, there was no optimal exposure time for the chip-prototype as the NO₂⁻-N SARR inhibition was never sufficient to achieve stable PN.

Biofilm characteristics

Biofilm characteristics measured in this study for the thin and thick biofilm carriers at 20 °C include the biofilm mass (Figure 2(a)), thickness (Figure 2(b)), and morphology (Supplementary Figure S4a,b). The average biofilm mass measurements were 1.7 ± 0.23 and 17 ± 1.58 mg biofilm/carrier for the thin and thick biofilm carriers, respectively (Table 2). Note the average biofilm mass measurements were obtained by measuring the biofilm mass of a batch of 20 carriers simultaneously, the error was not calculated. The biofilm thickness measurements were 38 ± 2.55 and 319 ± 10.87 μm for the thin and thick biofilm carriers, respectively (Table 2). The thick biofilm carrier had an order of magnitude larger biofilm thickness and biofilm mass per carrier than the z-prototype carrier. The morphology of the thin biofilm carrier had a thin, irregular biofilm that was thicker near the carrier walls and thinner near the middle of the carrier cells. There was also biofilm growth on a portion of the carrier walls that were unprotected; however, the biofilm was very thin. The thick biofilm carrier biofilm was very thick, and many of the carrier pores were clogged. The thin and thick biofilm carriers were exposed to the same shear, with an average velocity gradient G of 216 s⁻¹ (Supplementary eqns S1 and S2). This mixing velocity is greater than the minimum mixing velocity of 185 s⁻¹ found by Garcia (2016) who operated a similar system; however, the velocity gradient used during the batch tests was on the low end of velocity gradient ranges conventionally used (Melcer 2015; Garcia 2016). Thus, the mixing within the reactor did not provide significant biofilm thickness loss.

The biofilm thickness and biofilm mass per carrier for the thick biofilm carrier were an order of magnitude greater than the biofilm thickness and biofilm mass per carrier for the thin biofilm carrier. The surface areas for the thin and thick biofilm carriers were very similar and had similar biofilm thickness: mass ratios; thus, the two carrier types had similar biofilm densities. This similarity in biofilm density is in contrast to what has been seen in the literature where an increase in biofilm thickness is often associated with a decrease in biofilm density (Piculell *et al.* 2015; Schopf *et al.* 2019). This difference in biofilm characteristics yet similar biofilm densities between the thin and thick biofilm carriers is due to the significant difference in carrier geometry while operating at conventional loading rates where the carriers are not excessively stressed as

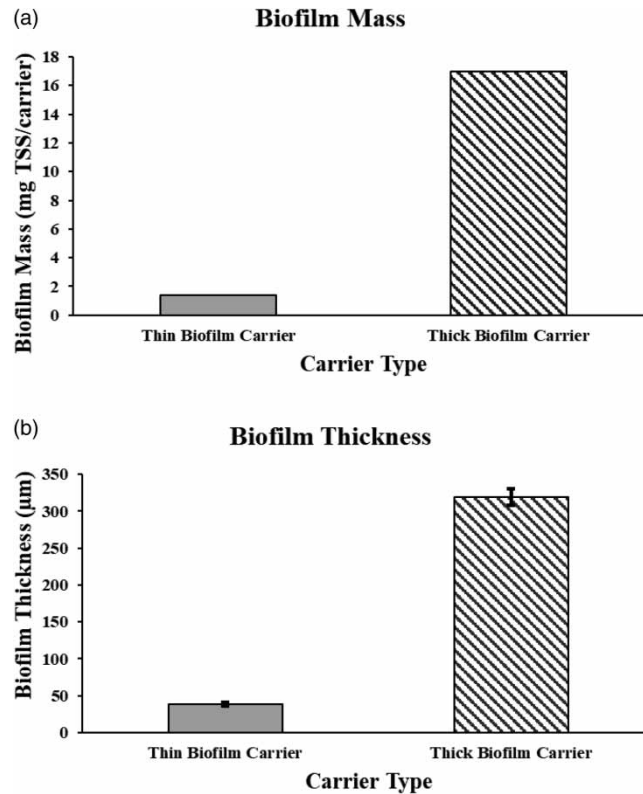


Figure 2 | Biofilm mass (a) and biofilm thickness (b) for the thin biofilm carrier (dark gray) and thick biofilm carrier (hatched).

Table 2 | Biofilm mass and thickness of the thin and thick biofilm carriers

Carrier type	Biofilm mass (mg TSS/carrier)	Biofilm thickness (μm)
Thin biofilm carrier	1.7 ± 0.23	38 ± 2.55
Thick biofilm carrier	17 ± 1.58	319 ± 10.87

biofilm stress has been shown to increase biofilm thickness and reduce density (Flemming 1993; White & Gadd 2000; Bjornberg *et al.* 2009).

To compare the approximate bacterial activity of the thin and thick biofilm carriers, the normalized AOB and NOB activity rates were calculated. The normalized AOB and NOB activity rates can be approximated using baseline nitrification kinetics, biofilm thickness (Table 3), and biofilm mass (Table 4) and will be represented as SARR/μm or SARR/mg biofilm where SARR is expressed using units of g N/m²·d. The thin biofilm carrier had more than five times higher AOB activity and more than two times higher NOB activity per biofilm mass or per biofilm thickness than the thick biofilm carrier. This difference in activity could be due to the bacterial density of the biofilm and the theory that only a portion of the biofilm is used for any one process and that only the top layer of the biofilm is most active (Liu & Capderville 1994); therefore, the most active portion of the biofilm is the entirety of the thin biofilm but only a portion of the thick biofilm volume; therefore, the activity efficiency of the thin biofilm carrier would be higher (Liu & Capderville 1994; Torresi *et al.* 2016).

Table 3 | Baseline AOB and NOB activity normalized for biofilm thickness

Carrier type	AOB activity (SARR/μm thickness)	NOB activity (SARR/μm thickness)
Thin biofilm carrier	0.0375	0.0366
Thick biofilm carrier	0.0067	0.0158

Table 4 | Baseline AOB and NOB activity normalized for biofilm mass

Carrier type	AOB activity (SARR/mg biomass)	NOB activity (SARR/mg biomass)
Thin biofilm carrier	0.838	0.818
Thick biofilm carrier	0.151	0.355

Activity rates in biofilm systems are diffusion rate-limited rather than rate-limited as sessile bacteria only have access to substrate that has diffused through the biofilm unlike planktonic bacteria that have access to substrate in the bulk fluid. Likewise, diffusion limitations can influence the impact of inhibitors on the microbiome as the inhibitor needs to diffuse through the biofilm to have contact with the microbiome; therefore, a thicker biofilm has been shown to reduce the impact of inhibitors compared to thinner biofilms (Flemming 1993). In the present study, it has been shown that both the thick biofilm AOB and NOB activity experienced less inhibition than the thin AOB and NOB activity, which follows the literature trends.

Microbiome

The microbiomes are analyzed by quantifying the percent abundance along with the Shannon and Simpson alpha-diversity indexes. Table 5 presents the top 20 most abundant genera of the thick biofilm carriers and thin biofilm carriers, which had a total of 465 and 403 observed OTUs, respectively. The top 20 most abundant genera account for 71.4% of the total abundance in the thick biofilm carrier microbiome, while the top 20 most abundant genera account for 80.5% of the total abundance in the thin biofilm carrier microbiome. *Nitrosomonas* was the second most abundant bacteria for both the thick and thin biofilms at relative abundances of 10.2 and 11.2%, respectively. *Nitrospira* was the third most abundant bacteria for the thick biofilm (9.5%); however, *Nitrospira* was only the 16th most abundant bacteria for the thin biofilm (1.2%). The difference in *Nitrospira* abundance and biofilm mass, due to the difference in carrier geometry and as a result biofilm thickness, could be a reason that the NO₂⁻-N SARR is higher in the thick biofilm than the thin biofilm. The most abundant genus in

Table 5 | Top 20 most abundant bacteria for the thick and thin biofilm carriers

Genus	Thick biofilm abundance (%)	Thin biofilm abundance (%)
<i>Nitrosomonas</i>	10.24	11.19
<i>Xanthomonas</i>	12.99	4.45
<i>Hyphomicrobium</i>	4.07	12.26
<i>Defluviimonas</i>	3.40	7.94
<i>Nitrospira</i>	9.48	1.22
f_Anaerolineaceae_OTU_12	5.55	4.73
<i>Devosia</i>	2.31	7.15
<i>Rhodobacter</i>	4.10	4.53
f_Sphingomonadaceae_OTU_36	1.48	4.07
<i>Planctomyces</i>	1.44	4.01
<i>Pedomicrobium</i>	1.76	3.27
o_DB1-14_OTU_28	3.39	0.94
MNG7	0.85	3.21
<i>Meganema</i>	0.92	2.87
f_Phyllobacteriaceae_OTU_15	1.53	2.03
<i>Pirellula</i>	1.25	2.16
f_Saprosiraceae_OTU_153	2.86	0.21
<i>Bosea</i>	0.10	2.82
f_Anaerolineaceae_OTU_86	1.52	1.18
f_Chitinophagaceae_OTU_69	2.19	0.27

the thick biofilm was *Xanthamonas* (13%), which has been theorized to be involved in TAN oxidation (Dosta *et al.* 2015). The most abundant genus in the thin biofilm was *Hyphomicrobium* (12.3%), which is a heterotroph that is most likely a result of the organic carbon present in the diluted centrate used for continuous operations.

The alpha-diversity (Figure 3) is a representation of the diversity within the microbiome. The Shannon index represents both the richness (numbers of different bacteria) and the evenness (abundance of each bacterium), while the Gini-Simpson index represents dominance as it does not take into account the richness, only the evenness and total number of organisms without distinguishing between species. The Shannon index values of the thick and thin biofilms are 4.05 and 3.92, respectively; therefore, the thick biofilm had a similar Shannon index diversity to the thin biofilm. The Shannon index values are lower than the values seen from nitrifying MBBR operating at a municipal wastewater treatment plant pilot study (Suarez *et al.* 2019). This difference in diversity may be due to the difference in source waters as in this study the water source is diluted centrate, while the pilot study used a constantly changing municipal wastewater. The thick biofilm and thin biofilm had Gini-Simpson indices of 0.954 and 0.962 where 0 represents a single bacteria system and 1 represents the maximum diversity, thus demonstrating that the systems have similar diversities. These Gini-Simpson index values are similar to other nitrifying biofilm systems (Jia *et al.* 2018; Wang *et al.* 2018). The difference in results from the Shannon and the Gini-Simpson index is most likely due to how the indexes were calculated and what they represent. Although the diversity indices are very similar for the thick and thin biofilm carriers, the thick biofilm shows 465 observed OTUs, while the thin biofilm shows 403 observed OTUs, demonstrating that the thick biofilm has a higher richness. Conversely, the top 10 most abundant bacteria account for 58.4 and 54.6% of the total abundance for the thick biofilm and thin biofilm, respectively, demonstrating that the thin biofilm has a higher evenness, despite similar diversities.

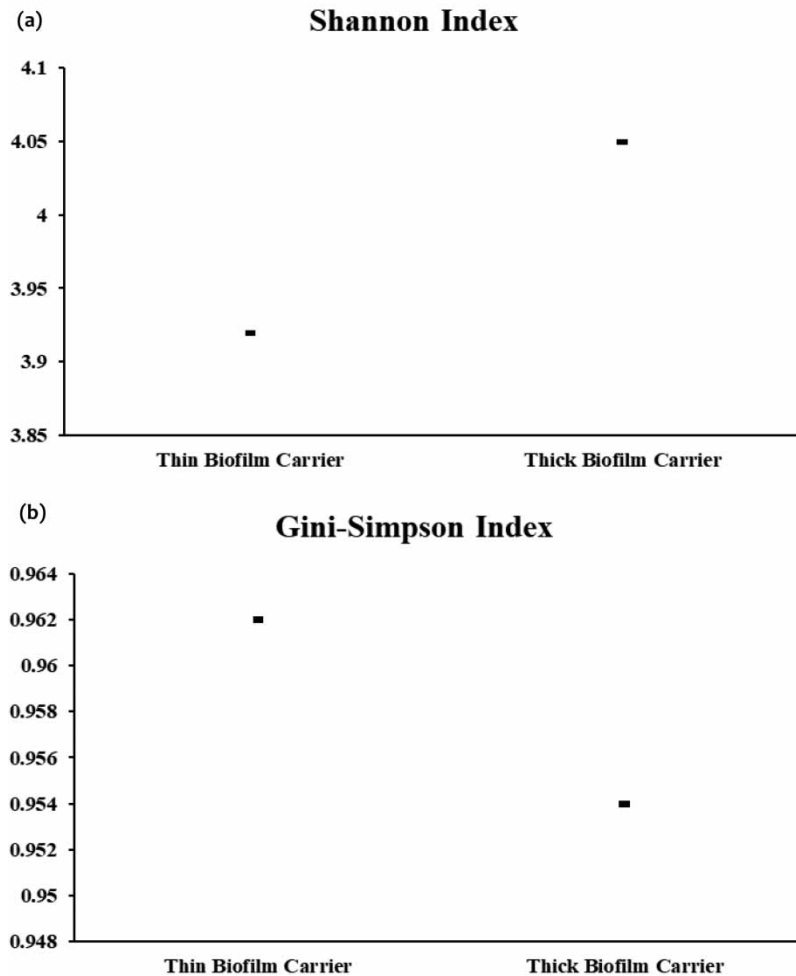


Figure 3 | Shannon (a) and Gini-Simpson (b) alpha-diversity indexes for thick and thin biofilm carriers.

The thick biofilm carrier had higher baseline TAN SARR and NO_2^- -N SARR kinetics than the thin biofilm carrier. The thick biofilm experienced a very different response to FNA than the thin biofilm, as stable PN was not achieved with the thick biofilm even after 4 h of exposure to the synthetic centrate solution. Conversely, sufficient PN (93% NO_2^- -N SARR inhibition) was achieved with the thin biofilm after 3 h of exposure, and PN (100% NO_2^- -N SARR inhibition) was achieved with the thin biofilm after 4 h of exposure to the synthetic centrate. Furthermore, both the thick and thin biofilms maintained significant TAN SARR kinetics; however, the thin biofilm experienced greater percentage TAN SARR inhibition than the thick biofilm even with similar abundances of *Nitrosomonas*. Therefore, the carrier design has a significantly greater effect on an inhibition response than the microbiome. This is likely due to the fact that the biofilm on the thick biofilm carrier was allowed to grow unrestricted and, therefore, became very thick, while the thin biofilm carrier, by design, defined the maximal biofilm thickness and, therefore, had a very thin biofilm. This difference in biofilm thickness and mass is likely the defining factor for inhibition effects as well as microbiome populations. The difference in biofilm thicknesses causes differences in the substrate and inhibitory exposure of the microbiomes due to diffusion limitations of the biofilms. Diffusion limitations in biofilms result in a concentration gradient of substrate and inhibitors within the biofilm and can result in zones of different oxygen states such as oxic and anoxic, as well as limiting exposure to inhibitors. The thick biofilm has a greater thickness than the thin biofilm; thus, the bacteria deeper in the biofilm are less likely to experience FNA inhibition, and this may have contributed to the difference in the inhibition effects observed. Biofilm thickness can also impact substrate penetration, especially oxygen penetration; however, due to the relatively high *Nitrospira* abundance and NOB activity with the thick biofilm, it is unlikely that the depth of oxygen penetration caused a significant impact on the biofilms. This study shows that carrier geometry-controlled biofilm thickness is likely a preferential strategy for achieving consistent PN.

CONCLUSIONS

Undefined biofilm thickness (thick biofilm carrier/chip-prototype) versus defined maximal biofilm thickness (thin biofilm carrier/z-prototype) carrier design strategies were investigated through batch testing to determine the ideal biofilm thickness definition strategy for achieving PN using FNA exposure. Through batch testing, it was found that the ideal biofilm thickness strategy was to use a defined maximal biofilm thickness strategy because only the thin biofilm was able to achieve complete NOB inhibition at the FNA exposure times tested. The thin biofilm carrier at 20 °C was able to achieve PN after 3 h of exposure to 0.88 mg FNA/L, while the thick biofilm carrier was unable to achieve stable PN without further nitrification during the batch tests even at 4 h of exposure. In addition, there was no clear indication that further exposure would have allowed the chip-prototype to achieve complete NOB inhibition with maintained stable nitritation, likely due to the extent that the biofilm thickness was able to be achieved.

ACKNOWLEDGEMENTS

The authors would like to acknowledge AnoxKaldnes and the NSERC CREATE TECHNOMISE program for the opportunity to perform this research and for support throughout the experiment.

FUNDING

Funding for this project was provided by AnoxKaldnes and the NSERC CREATE TECHNOMISE program.

CONFLICTS OF INTEREST

The authors are not aware of any conflicts of interest.

DATA AVAILABILITY STATEMENT

All relevant data are included in the paper or its Supplementary Information.

REFERENCES

- Albertsen, M., Karst, S. M., Ziegler, A. S., Kirkegaard, R. H. & Nielsen, P. H. 2015 [Back to basics – the influence of DNA extraction and primer choice on phylogenetic analysis of activated sludge communities](#). *PLoS ONE* **10**, e0132783.
- Anthonisen, A. C., Loehr, R. C., Prakasam, T. B. S. & Srinath, E. G. 1976 Inhibition of nitrification by ammonia and nitrous acid. *Water Pollution and Control Federation* **48**, 835–852.

- Bjornberg, C., Lin, W. & Zimmerman, R. A. 2009 Effect of temperature on biofilm growth dynamics and nitrification in a full-scale MBBR system. *Proceedings of the Water Environment Federation, WEFTEC 2009: Session 61 through 70*, pp. 4407–4426.
- Bolger, A. M., Lohse, M. & Usadel, B. 2014 Trimmomatic: a flexible trimmer for Illumina sequence data. *Bioinformatics* **30**, 2114–2120.
- Caporaso, J. G., Kuczynski, J., Stombaugh, J., Bittinger, K., Bushman, F. D., Costello, E. K., Fierer, N., Peña, A. G., Goodrich, J. K., Gordon, J. I., Huttley, G. A., Kelley, S. T., Knights, D., Koenig, J. E., Ley, R. E., Lozupone, C. A., McDonald, D., Muegge, B. D., Pirrung, M., Reeder, J., Sevinsky, J. R., Turnbaugh, P. J., Walters, W. A., Widmann, J., Yatsuneko, T., Zaneveld, J. & Knight, R. 2010 QIIME allows analysis of high-throughput community sequencing data. *Nature Methods* **7**, 335–336.
- Caporaso, J. G., Lauber, C. L., Walters, W., Berg-Lyons, D., Huntley, J., Fierer, N., Owens, S. M., Betley, J., Fraser, L., Bauer, M., Gormley, N., Gilbert, J. A., Smith, G. & Knight, R. 2012 Ultra-high throughput microbial community analysis on the Illumina HiSeq and MiSeq platforms. *The ISME Journal* **6**, 1621–1624.
- Christensson, M., Ekström, S., Anderson Chan, A., Le Vaillant, E. & Lemaire, R. 2013 Experience from start-ups of the first ANITA Mox plants. *Water Science and Technology* **67** (12), 2677–2684.
- Dosta, J., Vila, J., Sancho, I., Basset, N., Grifoll, M. & Mata-Alvarez, J. 2015 Two-step partial nitrification/Anammox in granulation reactors: start-up operation and microbial characterization. *Journal of Environmental Management* **164**, 196–205.
- Duan, H., Ye, L., Lu, X. & Yuan, Z. 2019 Overcoming nitrite oxidizing bacteria adaptation through alternating sludge treatment with free nitrous acid and free ammonia. *Environmental Science and Technology* **53** (4), 1937–1946.
- Edgar, R. C. 2013 UPARSE: highly accurate OTU sequences from microbial amplicon reads. *Nature Methods* **10**, 996–998.
- Flemming, H. C. 1993 Biofilms and environmental protection. *Water Science and Technology* **27**, 1–10.
- Fux, C., Huang, D., Monti, A. & Siegrist, H. 2004 Difficulties in maintaining long-term partial nitrification of ammonium-rich sludge digester liquids in a moving-bed biofilm reactor (MBBR). *Water Science and Technology* **49**, 53–60.
- Garcia, K. 2016 *The Effect of Biofilm Carrier Length on Nitrification in Moving bed Biofilm Reactors: an Examination of Mixing Intensity, Shock Loadings, and pH Changes*. Thesis. Available from: https://digitalrepository.unm.edu/ce_etds/115 (accessed 27 March 2021).
- Gilbert, E. M., Agrawal, S., Schwartz, T., Horn, H. & Lackner, S. 2015 Comparing different reactor configurations for partial nitrification/anammox at low temperatures. *Water Research* **81**, 92–100.
- Hellinga, C., Schellen, A. A. J. C., Mulder, J. W., van Loosdrecht, M. C. M. & Heijnen, J. J. 1998 The SHARON process: an innovative method for nitrogen removal from ammonium-rich waste water. *Water Science and Technology* **37**, 135–142.
- Jia, W., Chen, Y., Zhang, J., Li, C., Wang, Q., Li, G. & Yang, W. 2018 Response of greenhouse gas emissions and microbial community dynamics to temperature variation during partial nitrification. *Bioresour Technol* **261**, 19–27.
- Jumpstart Consortium Human Microbiome Project Data Generation Working Group 2012 Evaluation of 16 s rDNA-based community profiling for human microbiome research. *PLoS ONE* **7**, e39315.
- Lackner, S., Gilbert, E. M., Vlaemineck, S. E., Joss, A., Horn, H. & van Loosdrecht, M. C. M. 2014 Full-scale partial nitrification/anammox experiences – an application survey. *Water Research* **55**, 292–303.
- Lemaire, R., Zhao, H., Thomson, C., Christensson, M. & Piveteau, S. 2014 Mainstream deammonification with ANITA™ Mox process. In: *Proceedings of WEFTEC*, September 27–October 1, 2014, New Orleans, USA.
- Liu, Y. & Capdeville, B. 1994 Kinetics behaviors of nitrifying biofilm growth in wastewater nitrification process. *Environmental Technology* **15** (11), 1001–1013.
- Lotfi, K., Bonakdari, H., Ebtehaj, I., Mjalli, F. S., Zeynoddin, M., Delatolla, R. & Gharabaghi, B. 2019 Predicting wastewater treatment plant quality parameters using a novel hybrid linear-nonlinear methodology. *Journal of Environmental Management* **240**, 463–474. <https://doi.org/10.1016/j.jenvman.2019.03.137>.
- Magoč, T. & Salzberg, S. L. 2011 FLASH: fast length adjustment of short reads to improve genome assemblies. *Bioinformatics* **27**, 2957–2963.
- McIlroy, S. J., Kirkegaard, R. H., McIlroy, B., Nierychlo, M., Kristensen, J. M., Karst, S. M., Albertsen, M. & Nielson, P. H. 2017 MIDAS 2.0: an ecosystem-specific taxonomy and online database for the organisms of wastewater treatment systems expanded for anaerobic digester groups. *Database* **17**, bax016. <https://doi.org/10.1093/database/bax016>.
- Melcer, H. 2015 Mass transfer characteristics of floating media in MBBR and IFAS fixed-film systems. *Water Intelligence Online* **14**. doi:10.2166/9781780407050.
- Mulder, A. 2003 The quest for sustainable nitrogen removal technologies. *Water Science and Technology* **48**, 67–75.
- Piculell, M., Welander, P., Jönsson, K. & Welander, T. 2015 Evaluating the effect of biofilm thickness on nitrification in moving bed biofilm reactors. *Environmental Technology* **6**, 732–743.
- Piculell, M., Suarez, C., Chunyan, L., Christensson, M., Persson, F., Wagner, M., Hermansson, M., Jönsson, K. & Welander, T. 2016a The inhibitory effects of reject water on nitrifying populations grown at different biofilm thicknesses. *Water Research* **104**, 292–302.
- Piculell, M., Christensson, M., Jönsson, K. & Welander, T. 2016b Partial nitrification in MBBRs for mainstream deammonification with thin biofilms and alternating feed supply. *Water Science and Technology* **73** (6), 1253–1260.
- Quast, C., Pruesse, E., Yilmaz, P., Gerken, J., Schweer, T., Yarza, P., Peplies, J. & Glöckner, F. O. 2013 The SILVA ribosomal RNA gene database project: improved data processing and web-based tools. *Nucleic Acids Research* **41**, D590–D596.
- R Core Team 2017 *R: A Language and Environment for Statistical Computing*. R Foundation for Statistical Computing. Vienna, Austria.
- Rusten, B., Eikebrokk, B., Ulgenes, Y. & Lygren, E. 2006 Design and operations of the Kaldnes moving bed biofilm reactors. *Aquacultural Engineering* **34** (3), 322–331.

- Schopf, A., Delatolla, R. & Kirkwood, K. 2019 Partial nitrification at elevated loading rates: design curves and biofilm characteristics. *Biosystems and Bioprocess Engineering* **42**, 1809–1818.
- Shalini, S. & Joseph, K. 2012 Nitrogen management in landfill leachate: application of SHARON, Anammox, and combined SHARON-Anammox process. *Waste Management* **32** (12), 2385–2400.
- Siegrist, H., Salzberg, D., Eugster, J. & Joss, A. 2008 Anammox brings WWTP closer to energy autarky due to increased biogas production and reduced aeration energy for N-removal. *Water Science and Technology* **57** (3), 383–388.
- Strous, M., Heijnen, J. J., Kuenen, J. G. & Jetten, M. S. M. 1998 The sequencing batch reactor as a powerful tool to study very slowly growing micro-organisms. *Applied Microbiology and Biotechnology* **50**, 589–596.
- Suarez, C., Piculell, M., Modin, O., Langenheder, S., Persson, F. & Hermansson, M. 2019 Biofilm thickness matters: deterministic assembly of different functions and communities in nitrifying biofilms. *Scientific Reports*. doi:10.1038/s41598-019-41542-1.
- Third, K., Paxman, J., Schmid, M., Strous, M., Jetten, M. S. M. & Cord-Ruwisch, R. 2005 Enrichment of anammox from activated sludge and its application in the CANON process. *Microbial Ecology* **49**, 236–244.
- Torresi, E., Fowler, S. J., Polesel, F., Bester, K., Anderson, H. R., Smets, B. F., Plosz, B. G. & Christensson, M. 2016 Biofilm thickness influences biodiversity in nitrifying MBBRs – implications on micropollutant removal. *Environmental Science and Technology* **50**, 9279–9288.
- Van Loosedrecht, M. C. M. & Salem, S. 2006 Biological treatment of sludge digester liquids. *Water Science and Technology* **53** (12), 11–20.
- Wang, Q., Garrity, G. M., Tiedje, J. M. & Cole, J. R. 2007 Naive Bayesian classifier for rapid assignment of rRNA sequences into the new bacterial taxonomy. *Applied and Environmental Microbiology* **73**, 5261–5267.
- Wang, Z., Liang, H., Qu, F., Ma, J., Chen, J. & Li, G. 2013 Start-up of a gravity flow CANON-like MBR treating surface water under low temperature. *Chemical Engineering Journal* **217**, 466–474.
- Wang, Q., Ye, L., Jiang, G., Hu, S. & Yuan, Z. 2014 Side-stream sludge treatment using free nitrous acid selectively eliminates nitrite oxidizing bacteria and achieves the nitrite pathway. *Water Research* **55**, 245–255. doi:10.1016/j.watres.2014.02.029.
- Wang, C., Liu, S., Xu, X., Zhang, C., Wang, D. & Yang, F. 2018 Achieving mainstream nitrogen removal through simultaneous partial nitrification, anammox, and denitrification process in an integrated fixed film activated sludge reactor. *Chemosphere* **203**, 457–466.
- White, C. & Gadd, G. M. 2000 Copper accumulation by sulfate reducing bacterial biofilms. *FEMS Microbiology Letter* **183**, 313–318.
- Young, B., Delatolla, R., Abujamel, T., Kennedy, K., Laflamme, E. & Stintzi, A. 2017 Rapid start-up of nitrifying MBBRs at low temperatures: nitrification, biofilm response and microbiome analysis. *Bioprocess and Biosystems Engineering* **40** (5), 731–739. doi:10.1007/s00449-017-1739-5.

First received 6 July 2021; accepted in revised form 3 May 2022. Available online 13 May 2022